Scientific Research Publishing

Computational Water, Energy, and Environmental Engineering, 2023, 12, 1-26
https://www.scirp.org/journal/cweee
ISSN Online: 2168-1570
ISSN Print: 2168-1562

The Impact of Climate Change on the Stratification of Coastal Areas of the Euboean Gulf and the Diffusion of Urban Wastewater in Them

Evangelos Tsirogiannis, Panagiotis Angelidis

Division of Hydraulics, Department of Civil Engineering, School of Engineering, Democritus University of Thrace, Kimmeria Campus, Xanthi, Greece
Email: pangelid@civil.duth.gr

How to cite this paper: Tsirogiannis, E. and Angelidis, P. (2023) The Impact of Climate Change on the Stratification of Coastal Areas of the Euboean Gulf and the Diffusion of Urban Wastewater in Them. *Computational Water, Energy, and Environmental Engineering*, **12**, 1-26.
https://doi.org/10.4236/cweee.2023.123001

Received: May 18, 2023
Accepted: July 23, 2023
Published: July 26, 2023

Abstract

Hydrodynamic circulation in a marine environment, characterized by the influence of strong tides, atmospheric loading and bathymetry, is a complex phenomenon. The physical and hydrodynamic characteristics of this flow are absolutely crucial for the vertical mixing of the sea masses and consequently for the mixing of their physico-chemical parameters, such as nutrients and oxygen, as well as for the diffusion and dispersion of passive pollutants, the recharge of the waters and the general environmental situation. This paper examines the effect of a future increase in mean air temperature on the water column stratification of coastal areas of interest, which are subject to the above loadings and receive treated urban wastewater, and how this increase could affect their diffusion and mixing of conservative pollutants contained therein.

Keywords

3D Modelling, Stratification, Sewage, Euboean Gulf Greece, Climate Change

1. Introduction

The hydrodynamic circulation in coastal systems is often depending on various interacting processes such as tides, waves, and river inflows. Many researchers have spent their effort to model the effects of the tide [1]-[6]. Hydrodynamic processes significantly influence the mixing and transport of pollutants in coastal waters. Additionally, the tidal currents transport pollutants back and forth

before sometime dispersing them into the sea [7].

In the Eastern Mediterranean, the tidal currents are in general relatively weak and in most cases have low speeds [8]. One of the earliest historically observed tidal phenomenon is in the Gulf of Evoikos (Greece). Eratosthenes, Pitheas, Posidonios [9], Stravon and Senekas [10] have studied this phenomenon in antiquity and other researchers from the early 20th century [9]-[14]. Despite the fact that some research has been conducted in the wider southern European region [15] [16] [17] [18] on sea level changes, but also within the Euboean Gulf [19] [20], there are still today no systematic measurements and few available papers describing, explaining and illustrating the various effects of tides on hydrodynamic circulation, but also on the diffusion and transport of pollutants [21].

In the present study, the hydrodynamic circulation in the Euboean Gulf region was simulated by computer. The three-dimensional hydrodynamic model AEM3D (3-Dimensional coupled Hydrodynamic-Aquatic Ecosystem Model), which is the evolution of the ELCOM-CAEDYM software, was used. The AEM3D software is considered particularly effective for simulating hydrodynamic models that include the influence of the strong tides that characterize the study area, the Coriolis force—due to the rotation of the earth—and climatological factors such as total solar radiation, atmospheric pressure, relative humidity, precipitation, air temperature, wind speed and direction. This model also has been used very well in various relevant studies around the world, such as in the North Aegean Sea [22] [23], in the Adriatic Sea [24], in the Persian Gulf [25], a study in which also included a simulation of the tide and the Blagdon Lake in the UK, a study investigating the effect of climate change on stratification and the application of mitigation methods [26]. Special research regarding the hydrodynamic state of the Euboean Gulf and the conditions that affect, it has been conducted by Kotsovinos and Skaloumpakas [27] [28]. The *Mixing Characteristics under Tide, Meteorological and Oceanographic Conditions in the Euboean Gulf Greece* [29] has been simulated in a recent work of the author with the use of the AEM3D model. On the official website of the COPERNICUS system of climate change services (https://climate.copernicus.eu), an increase of 1.21˚C in the average global air temperature has been recorded since pre-industrial times, namely from 1970 to 2022. By the year 2034, if environmental conditions do not improve, a further increase in an average temperature of 0.29˚C is predicted. In other words, in the year 2034, an average increase in air temperature of 1.5˚C is expected, compared to 1970, as illustrated in the following **Figure 1**.

In this paper, a hypothetical climate scenario of a future increase in global air temperature of 1.5˚C is considered, assuming that in the next 64 years, there is no reversal of the greenhouse effect that is primarily responsible for this increase and that the average air temperature continues to rise at the same rate as in previous years.

The aim of the scenario and the present study is to simulate the increase in mean air temperature in order to investigate whether there will be more pronounced stratification at specific control points of coastal areas of interest, in

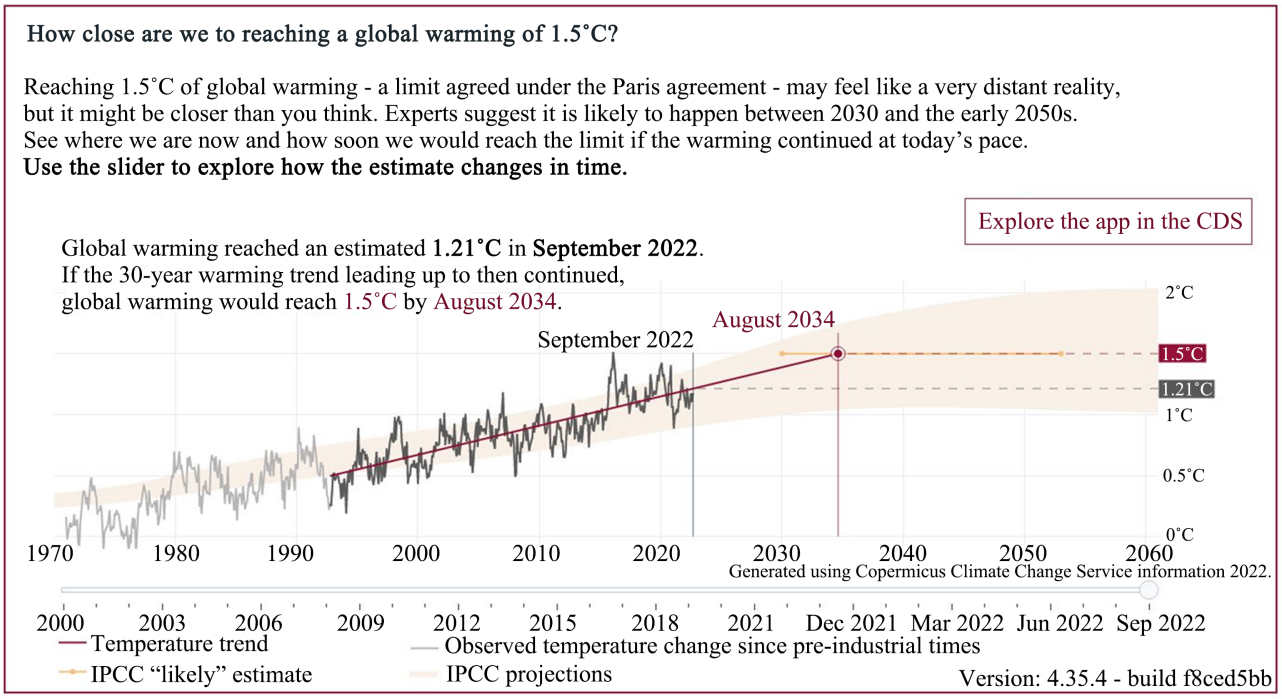

Figure 1. Increase in average global air temperature from the year 1970 to the year 2034, obtained from https://climate.copernicus.eu.

order to investigate whether and to what extent the possible increase in stratification will affect the hydrodynamic state of the lower bottom layers in coastal areas of interest, such as water temperature, flow rate, and water recharge time. The above characteristics are absolutely crucial for the vertical mixing of the sea masses and consequently for the mixing of their physico-chemical parameters, such as nutrients and oxygen, and consequently for the diffusion of urban wastewater from the disposal pipelines simulated in the computational domain of the study.

2. Methods

2.1. Study Area

The study area (**Figure 2**) consists of the North Euboean Gulf with a total area of 1060 Km^2 and the South Euboean Gulf with an area of 900 Km^2. The connection between these two bays is through the Euripus Strait, which is essentially a narrow and shallow channel with dimensions of 40 m × 40 m × 10 m, the main characteristic of which is the existence of a strong tide [20]. It is typically reported that during the half-period (T/2 = 6 h) the maximum flow rate in the Euripus Strait reaches about 2.5 m/s [27] [28].

2.2. Model Setup

The area of the Euboean Gulf, selected for the numerical simulation of the present study, whose bathymetry is shown in **Figure 3**. It is bounded to the west and east by Central Greece-Attica and Evia respectively, as well as by the northern

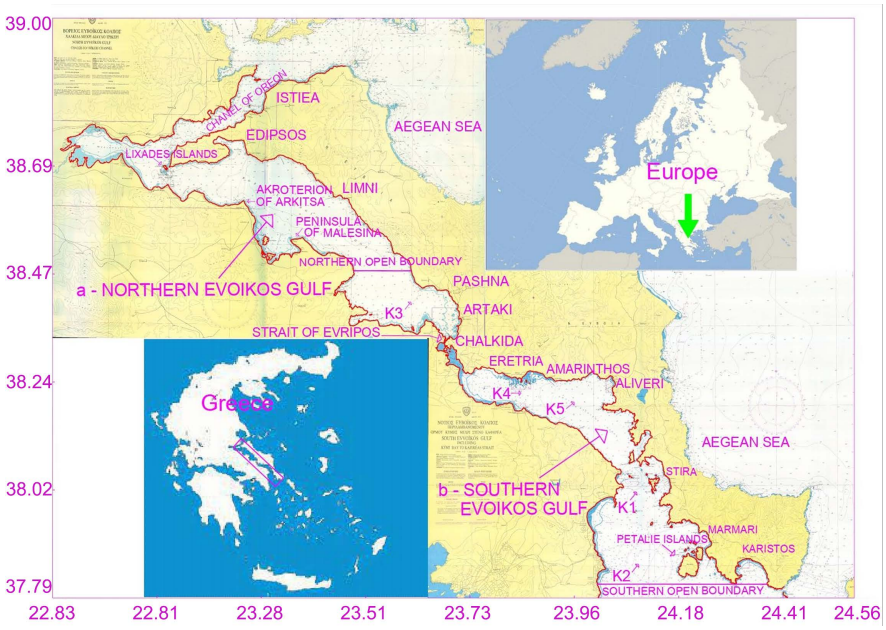

Figure 2. Map of the northern and the southern Gulf of Evoikos.

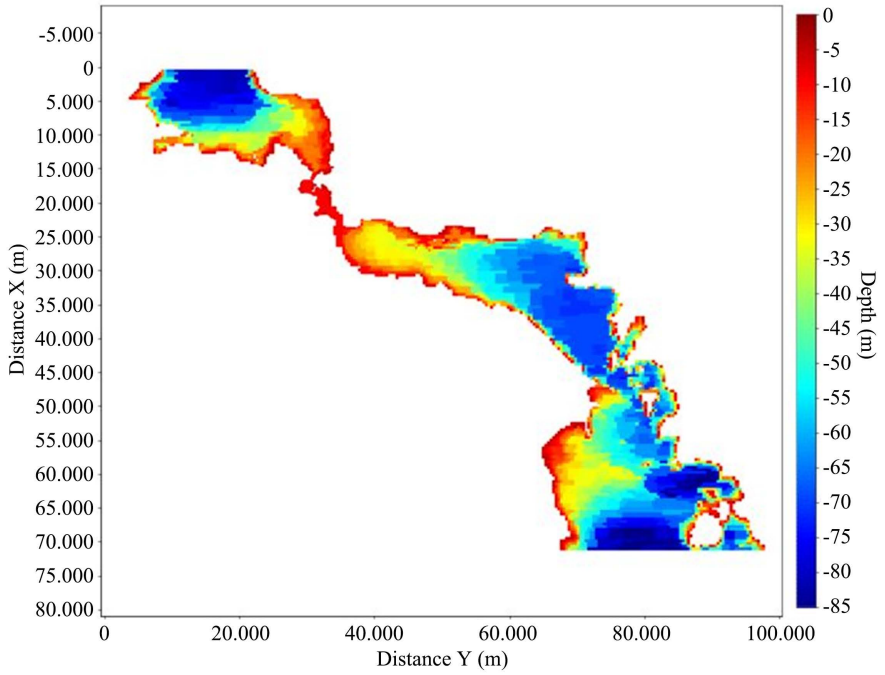

Figure 3. Bathymetric map of the simulation area of the Euboean Gulf.

and southern Aegean Sea. A variable-dimensional rectangular computational grid structured by rectangular computational discretization cells with dimensions of 40 m × 100 m to 400 m × 400 m was formed. The progressive variation of the dimensions of the computational cells was necessary due to the restrictive 40 m width of the Euripus Strait on the one hand and the avoidance of an excessive number of cells on the other hand in the case of using fixed 40 m × 40 m cells, which made it impossible to execute the computational code. Based on this

limitation, the computational simulation included the entire South Euboean Gulf and (1/3) the North Euboean Gulf. The northern and southern boundaries of the simulated area are shown in Figure 2.

A total of 20 layers were defined in the vertical direction. The first 8 layers from the surface were of variable thickness from 2.5 m to 5.0 m with a progressive increase, while the remaining 13 deeper layers up to the bottom had a constant thickness of 5.0 m. This vertical discretization by selecting as dense a vertical computational grid as possible was carried out in order: 1) to simulate as accurately as possible the hydrodynamic circulation of the 10 m deep Euripus Strait, which is absolutely crucial for the communication between the north and south Euboean Gulf; 2) to better reflect the results in the shallow coastal areas of particular interest; and 3) to achieve the highest possible accuracy in the vertical distribution of velocities, density stratification and tracer concentrations by depth. The maximum simulation depth reached −86.0 m. The computer network consisted of 225,351 active water cells.

A turbulent benthos boundary condition was used at the bottom by applying a constant friction coefficient. An "open" boundary condition was applied at the northern and southern boundary of the computational domain, passively allowing water to flow in or out of each cell according to the flow needs. Based on observations and measurements reported in the literature [14] [21] [27] [28], varying sea level boundary conditions were imposed on the northern and southern boundary to simulate tides, according to Figure 4.

The initial salinity and temperature condition at the start of the simulation in all cells of the computational domain was the same everywhere and equal to 38.88 psu and 18.35˚C respectively. These are average values for the year 2016, taken from the COPERNICUS system. The time step between cycles was 1.0 min. The simulation was performed for one year (2016) which was considered as a representative typical year. Meteorological data were fed in every 10 min, namely wind speed and direction, atmospheric pressure, air temperature, relative humidity, rainfall amount and solar radiation. These data (Figure 5) were measured by meteorological stations of the National Meteorological Service, located in the cities of Lamia and Aliarto, which are adjacent to the study area.

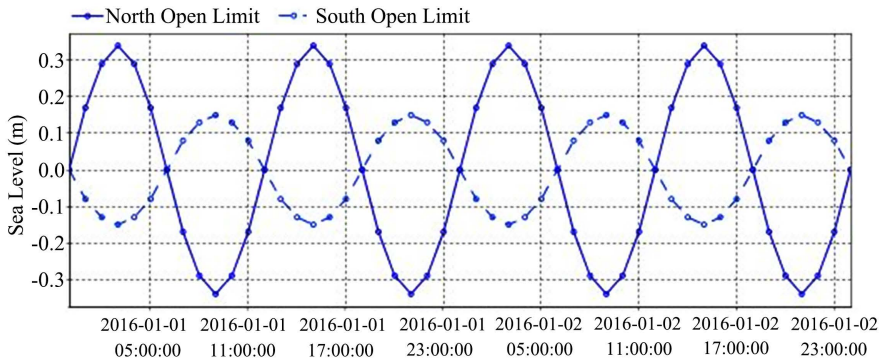

Figure 4. Tidal sea level variations at the northern and southern boundaries of the computational domain for 48 hours.

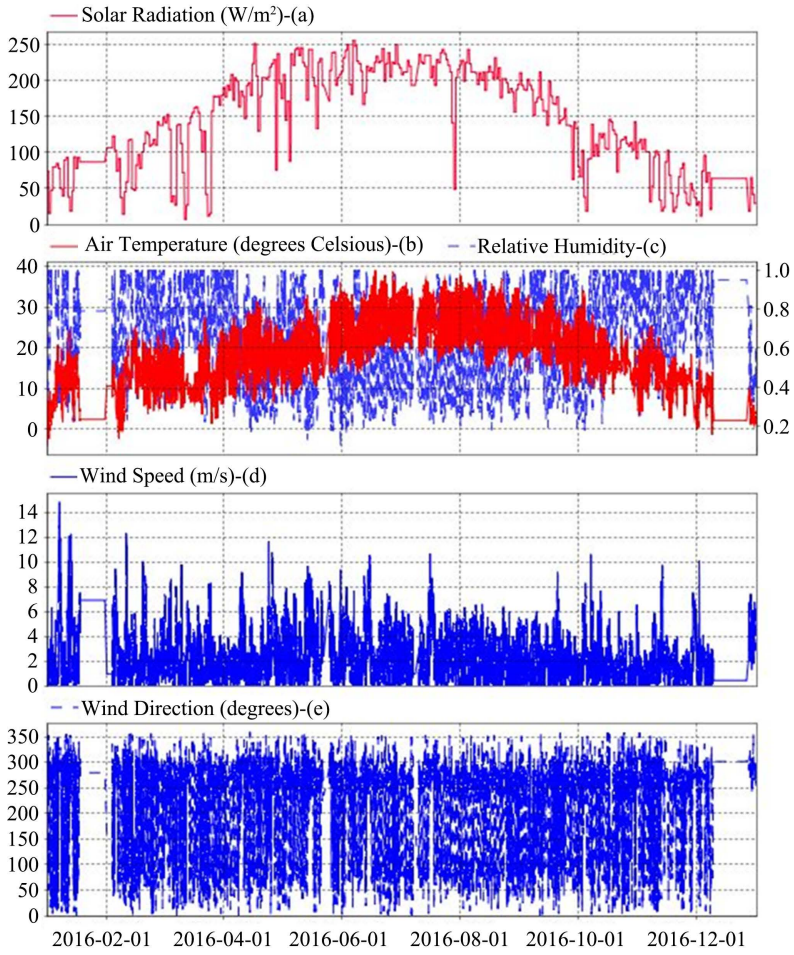

Figure 5. (a) Air temperature and solar radiation, (b) wind speed and direction, (c) atmospheric pressure and relative humidity, per 10 minutes for the year 2016 in the study area.

3. Results and Reliability

The validity of the results of the present study is first examined. Since there are no systematic field measurements in the study area, results of the present study will be compared with available COPERNICUS model predictions at two points K1 and K2 of the southern Euboean Gulf, whose location is shown in Figure 2.

Figures 6(a)-(d) show the time evolution of the mean salinity at different depths (1, 20, 40, 60 m), as obtained from the simulation of this study with the AEM3D software and from the COPERNICUS system at point K1. It is observed that the predictions of the two models are similar. The comparative results for point K2 and for depths of 1, 30, 50 and 80 m are similar (Figures 6(e)-(h)).

Figure 7 shows the comparison of the vertical distribution of the mean salinity, as a result of the simulation of the present study with the AEM3D software and as a prediction from the COPERNICUS system at point K2 for the months of August (Figure 7(a)) and December (Figure 7(b)). As can be seen, the simulation results with the two models are remarkably close. Similarly, the results of the two simulations are also similar at point K1 for various months considered.

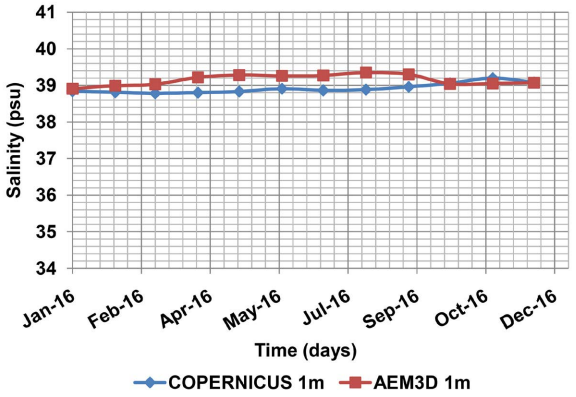
41
40
39
38
37
36
35
34
Salinity (psu)
Jan-16
Feb-16
Apr-16
May-16
Jul-16
Sep-16
Oct-16
Dec-16
Time (days)
COPERNICUS 1m
AEM3D 1m

(a)

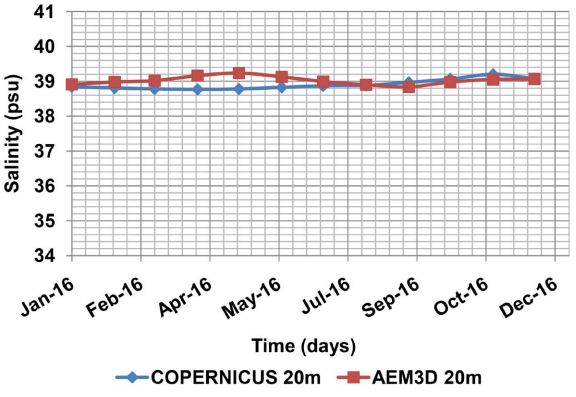
41
40
39
38
37
36
35
34
Salinity (psu)
Jan-16
Feb-16
Apr-16
May-16
Jul-16
Sep-16
Oct-16
Dec-16
Time (days)
COPERNICUS 20m
AEM3D 20m

(b)

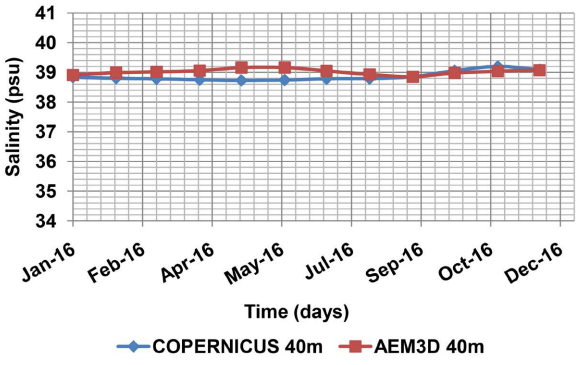
41
40
39
38
37
36
35
34
Salinity (psu)
Jan-16
Feb-16
Apr-16
May-16
Jul-16
Sep-16
Oct-16
Dec-16
Time (days)
COPERNICUS 40m
AEM3D 40m

(c)

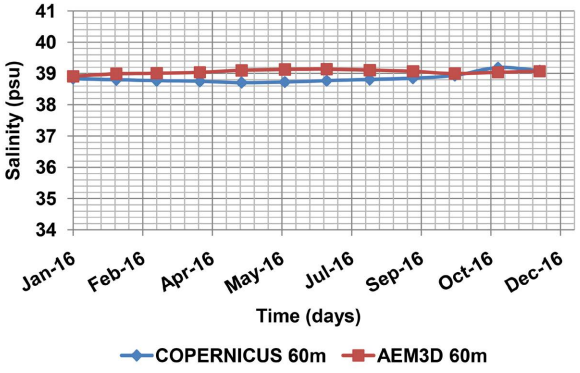
41
40
39
38
37
36
35
34
Salinity (psu)
Jan-16
Feb-16
Apr-16
May-16
Jul-16
Sep-16
Oct-16
Dec-16
Time (days)
COPERNICUS 60m
AEM3D 60m

(d)

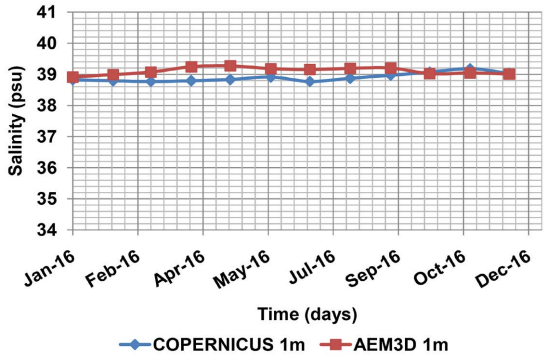

(e)

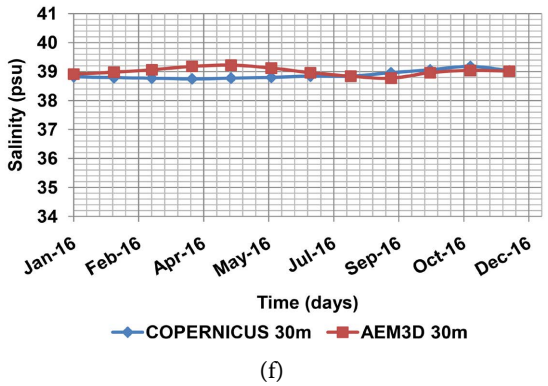

(f)

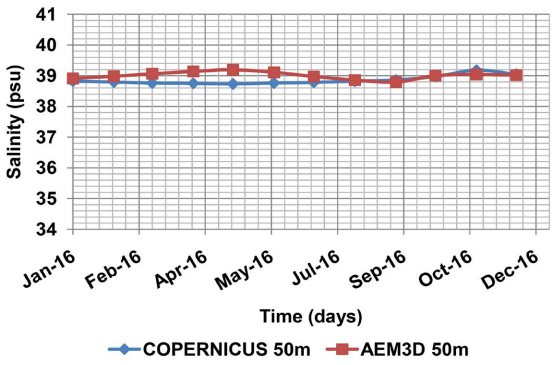

(g)

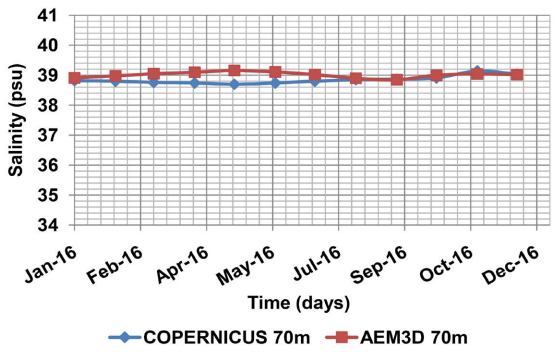

(h)

Figure 6. Comparison of the average salinity in a vertical water column for different depths, as obtained from the simulation of the present work by the AEM3D software and by the COPERNICUS system at points K1 ((a)-(d)) and K2 ((e)-(h)).

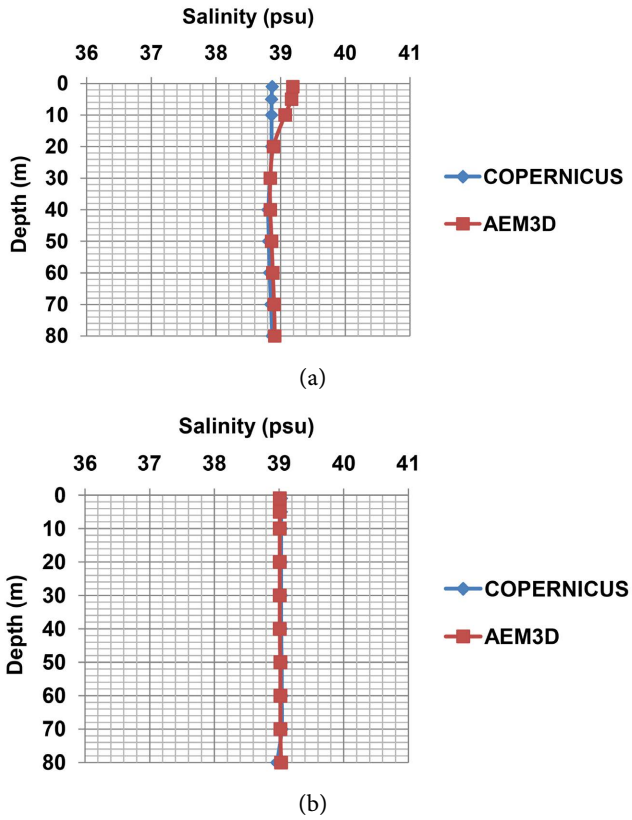

Figure 7. Comparison of the vertical distribution of the mean salinity, as obtained from the simulation of the present paper by the AEM3D software and by the COPERNICUS system at point K2 for the months of August (a) and December (b).

Figure 8 shows the time evolution of the mean temperature at point K1 for the surface (1 m depth) and for 10 m depth, based on the simulation of the present study with the AEM3D software and the COPERNICUS system prediction. For the whole simulation period of one year, the results of the two models converge satisfactorily [21].

Vertical distribution of the mean temperature at point K1 is shown in Figure 9(a) and Figure 9(b) for the months of May and June respectively. The comparison of the predictions of the present work with the AEM3D model and with the COPERNICUS system again shows satisfactory convergence [21].

4. Urban Wastewater Disposed of in the Area

Five (5) underwater pipelines for the disposal—through diffusers—of treated municipal wastewater are installed within the survey area [29]. Table 1 shows the names of the diffusers, the names of the areas where they are installed, the names of the corresponding tracers, the depth of disposal, the flow rate of the wastewater and the initial concentration of suspended solid particles contained in them. Figure 10 shows the locations of the underwater pipelines—diffusers as well as some of the control points (P1, P2, P3, P4, P5) defined in the framework of this research and Figure 11 shows in color the dimensionless concentration of

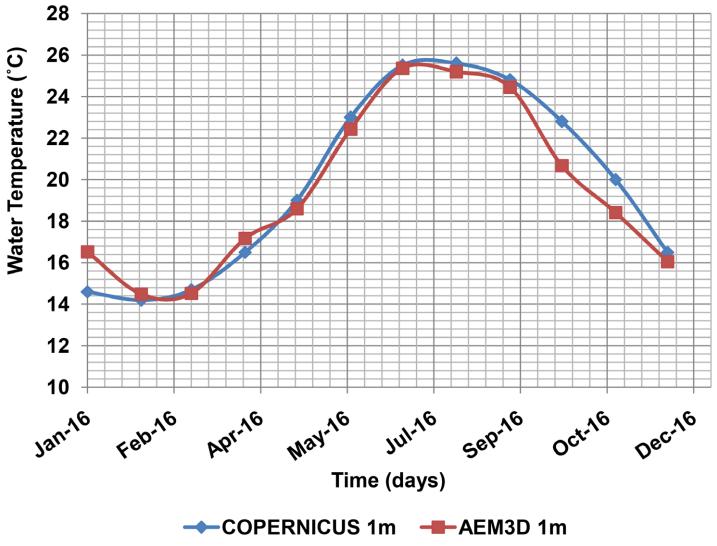

(a)

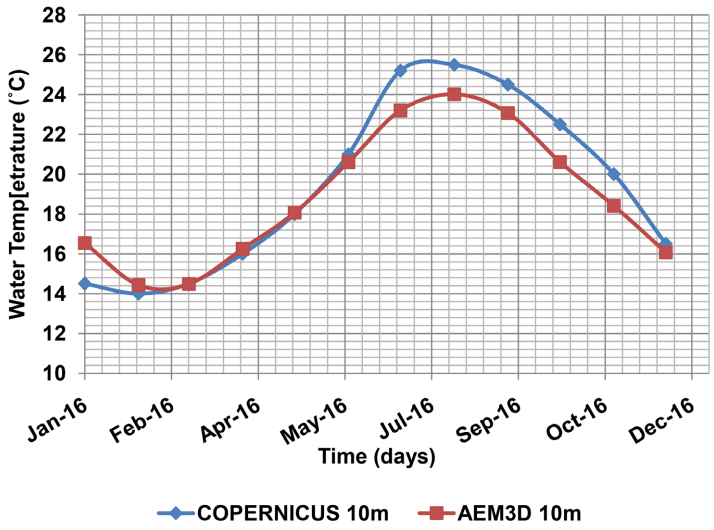

(b)

Figure 8. Temporal variation at point K1 of the mean temperature at the surface (depth 1 m) and at a depth of 10 m, as obtained from the simulation of the present study by the AEM3D software and the COPERNICUS system.

Table 1. Characteristics of disposal of treated urban waste water via diffusers.

No.	Diffuser's name	Setup Area	Tracer's name	Disposal depth (m)	Urban waste flow (m^3/s)	Concentration of suspended solid particles (mg/l)
1	DIFFUSER 1	KASTELA	Tracer 3	18	0.04	10
2	DIFFUSER 2	CHALKIS	Tracer 4	10	0.24	35
3	DIFFUSER 3	ERETRIA	Tracer 5	24	0.04	35
4	DIFFUSER 4	AMARINTHOS	Tracer 6	19	0.03	30
5	DIFFUSER 5	ALIVERI	Tracer 7	47	0.04	25

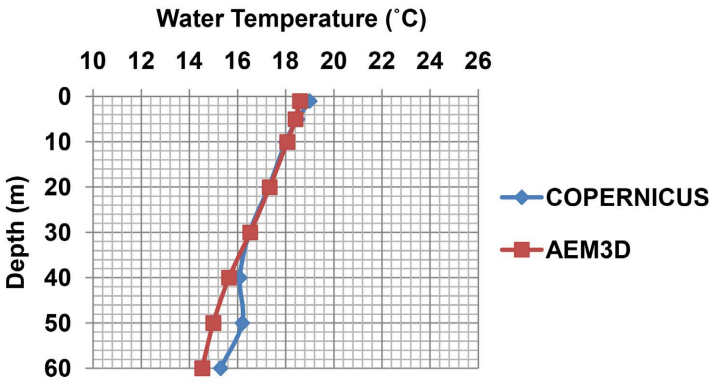

(a)

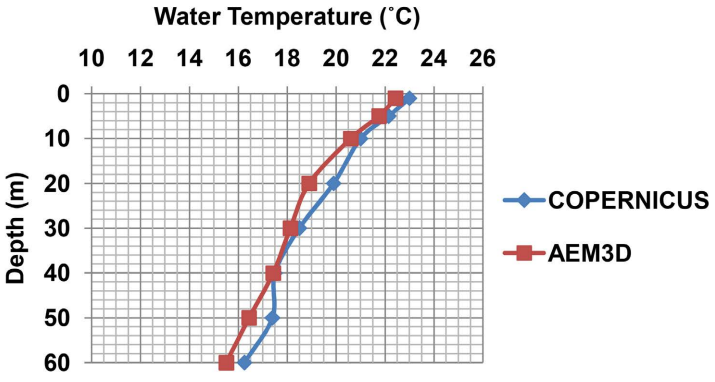

(b)

Figure 9. Comparison of the vertical distribution of the mean temperature, as obtained from the simulation of the present study by the AEM3D software and by the COPERNICUS system at point K1 for the months of May (a) and June (b).

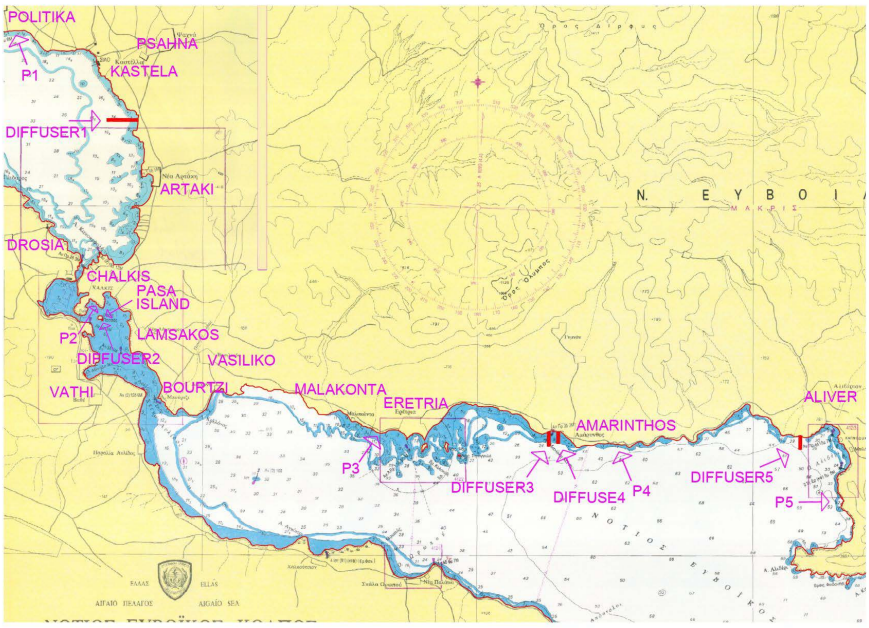

Figure 10. Positions of the underwater urban waste water disposal pipelines in the Euboean Gulf and the designated control sites in the coastal areas.

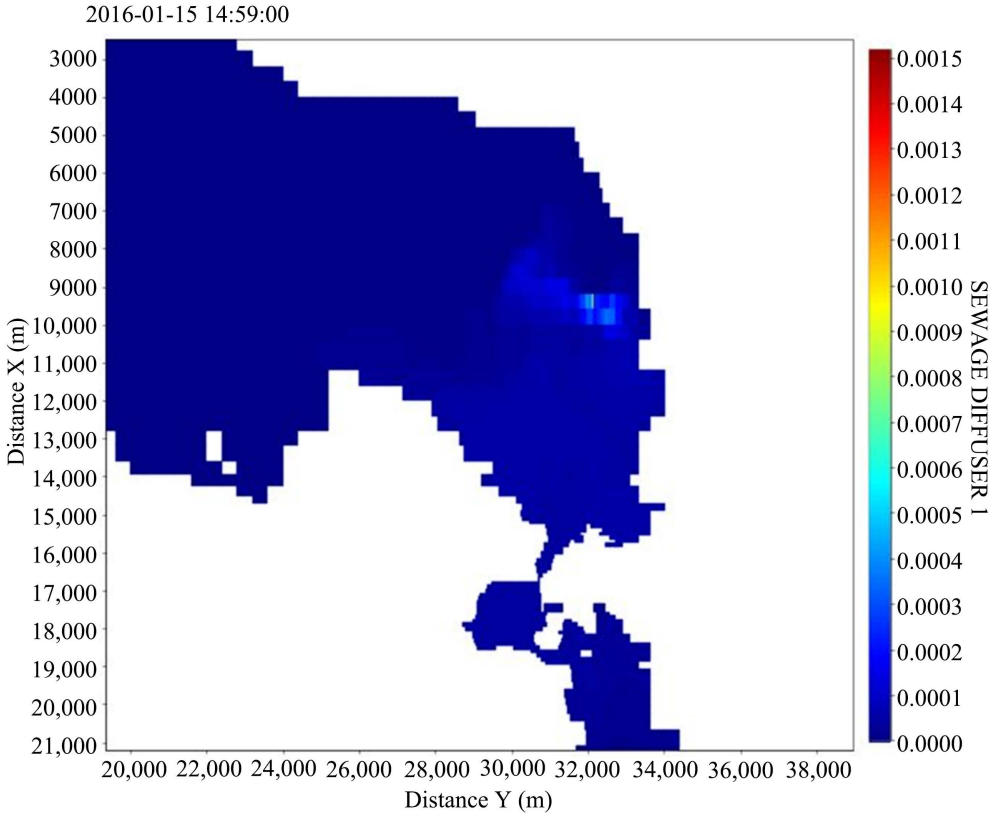
2016-01-15 14:59:00
Distance X (m)
3000
4000
5000
6000
7000
8000
9000
10,000
11,000
12,000
13,000
14,000
15,000
16,000
17,000
18,000
19,000
20,000
21,000
20,000 22,000 24,000 26,000 28,000 30,000 32,000 34,000 36,000 38,000
Distance Y (m)
0.0015
0.0014
0.0013
0.0012
0.0011
0.0010
0.0009
0.0008
0.0007
0.0006
0.0005
0.0004
0.0003
0.0002
0.0001
0.0000
SEWAGE DIFFUSER 1

(a)

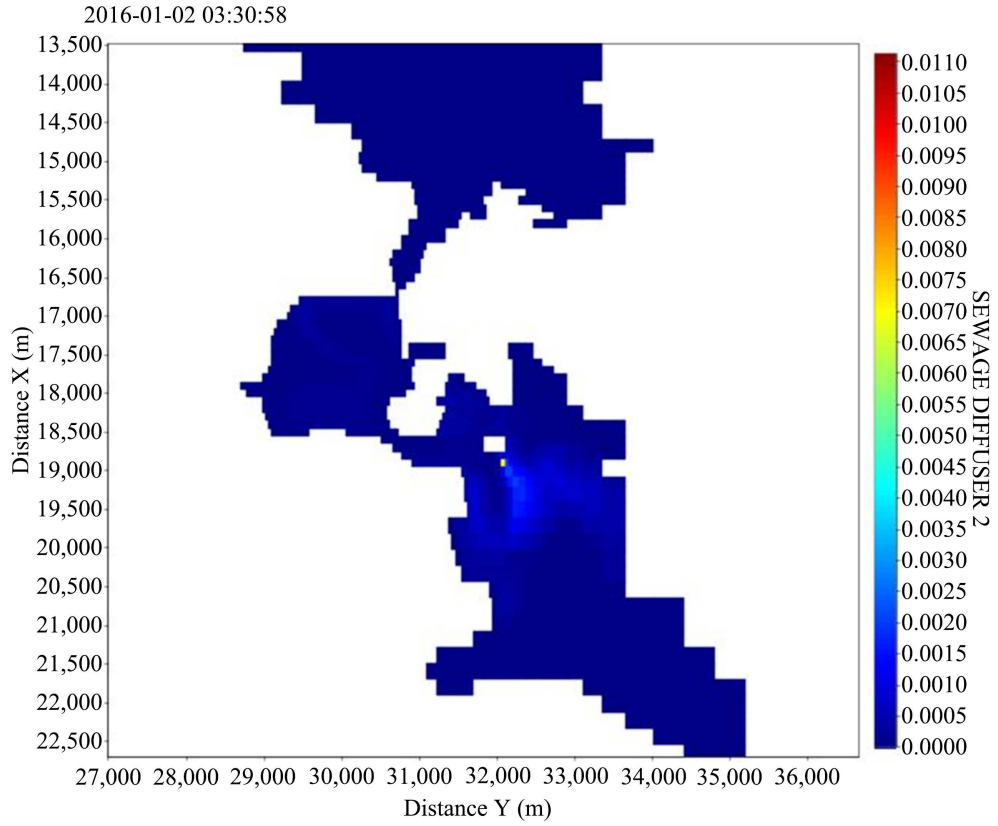
2016-01-02 03:30:58
Distance X (m)
13,500
14,000
14,500
15,000
15,500
16,000
16,500
17,000
17,500
18,000
18,500
19,000
19,500
20,000
20,500
21,000
21,500
22,000
22,500
27,000 28,000 29,000 30,000 31,000 32,000 33,000 34,000 35,000 36,000
Distance Y (m)
0.0110
0.0105
0.0100
0.0095
0.0090
0.0085
0.0080
0.0075
0.0070
0.0065
0.0060
0.0055
0.0050
0.0045
0.0040
0.0035
0.0030
0.0025
0.0020
0.0015
0.0010
0.0005
0.0000
SEWAGE DIFFUSER 2

(b)

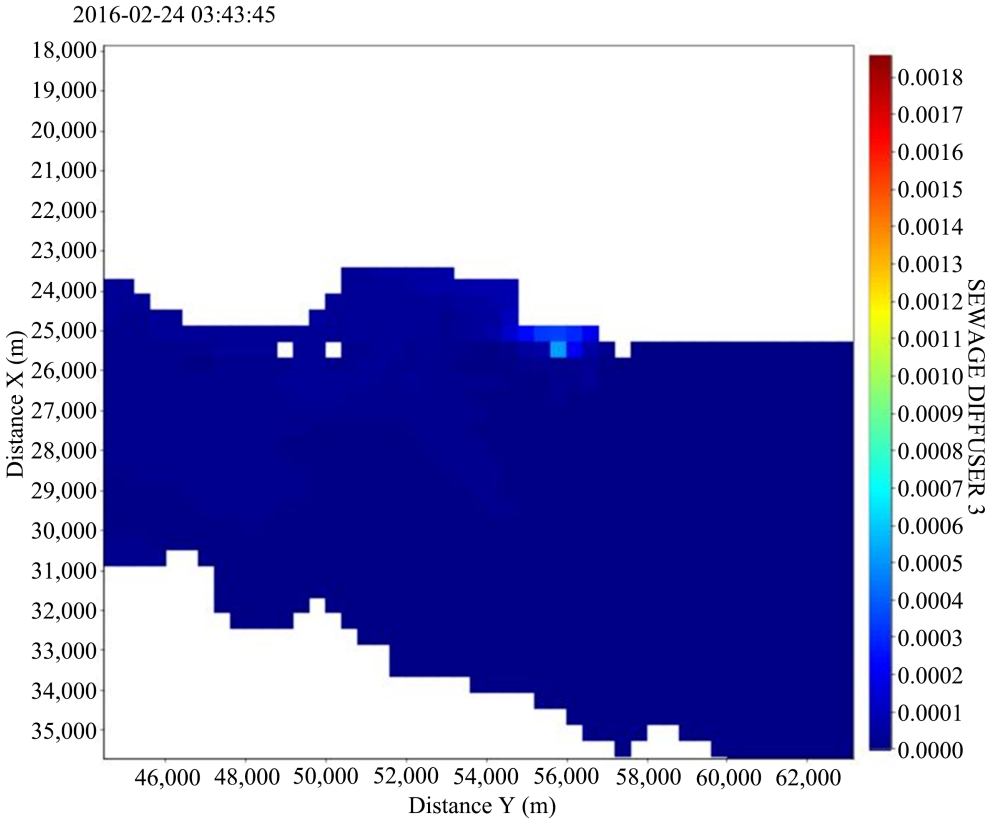
2016-02-24 03:43:45
Distance X (m)
18,000
19,000
20,000
21,000
22,000
23,000
24,000
25,000
26,000
27,000
28,000
29,000
30,000
31,000
32,000
33,000
34,000
35,000
46,000 48,000 50,000 52,000 54,000 56,000 58,000 60,000 62,000
Distance Y (m)
SEWAGE DIFFUSER 3
0.0018
0.0017
0.0016
0.0015
0.0014
0.0013
0.0012
0.0011
0.0010
0.0009
0.0008
0.0007
0.0006
0.0005
0.0004
0.0003
0.0002
0.0001
0.0000

(c)

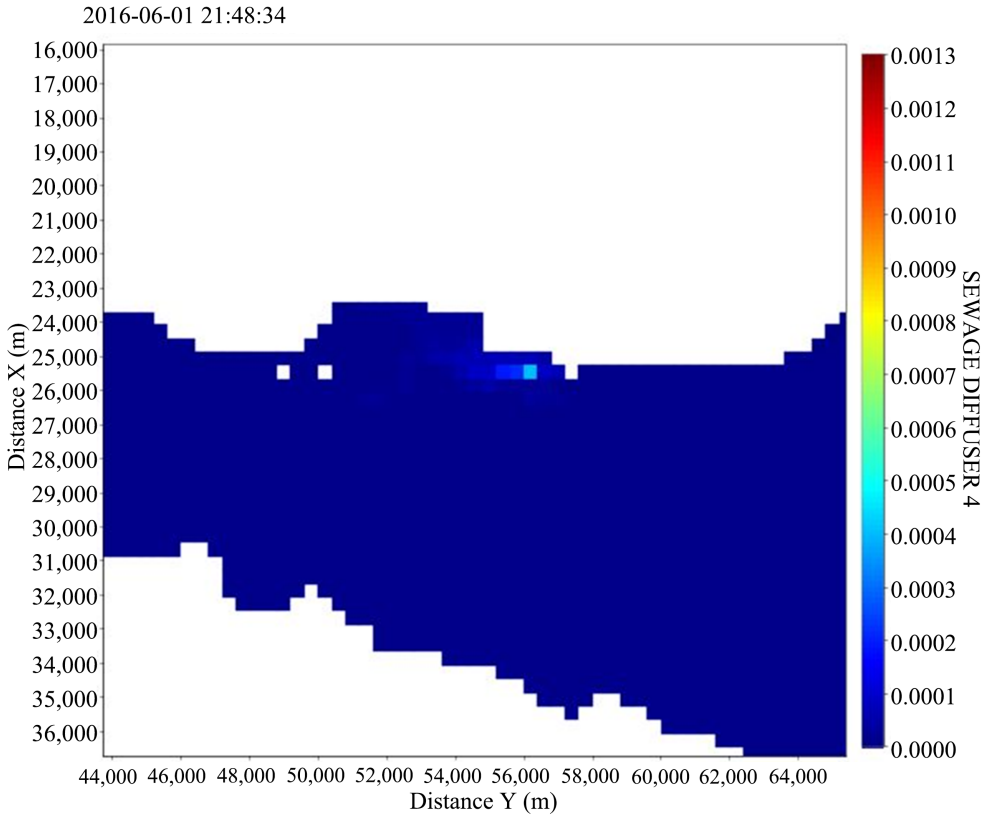
2016-06-01 21:48:34
Distance X (m)
16,000
17,000
18,000
19,000
20,000
21,000
22,000
23,000
24,000
25,000
26,000
27,000
28,000
29,000
30,000
31,000
32,000
33,000
34,000
35,000
36,000
44,000 46,000 48,000 50,000 52,000 54,000 56,000 58,000 60,000 62,000 64,000
Distance Y (m)
SEWAGE DIFFUSER 4
0.0013
0.0012
0.0011
0.0010
0.0009
0.0008
0.0007
0.0006
0.0005
0.0004
0.0003
0.0002
0.0001
0.0000

(d)

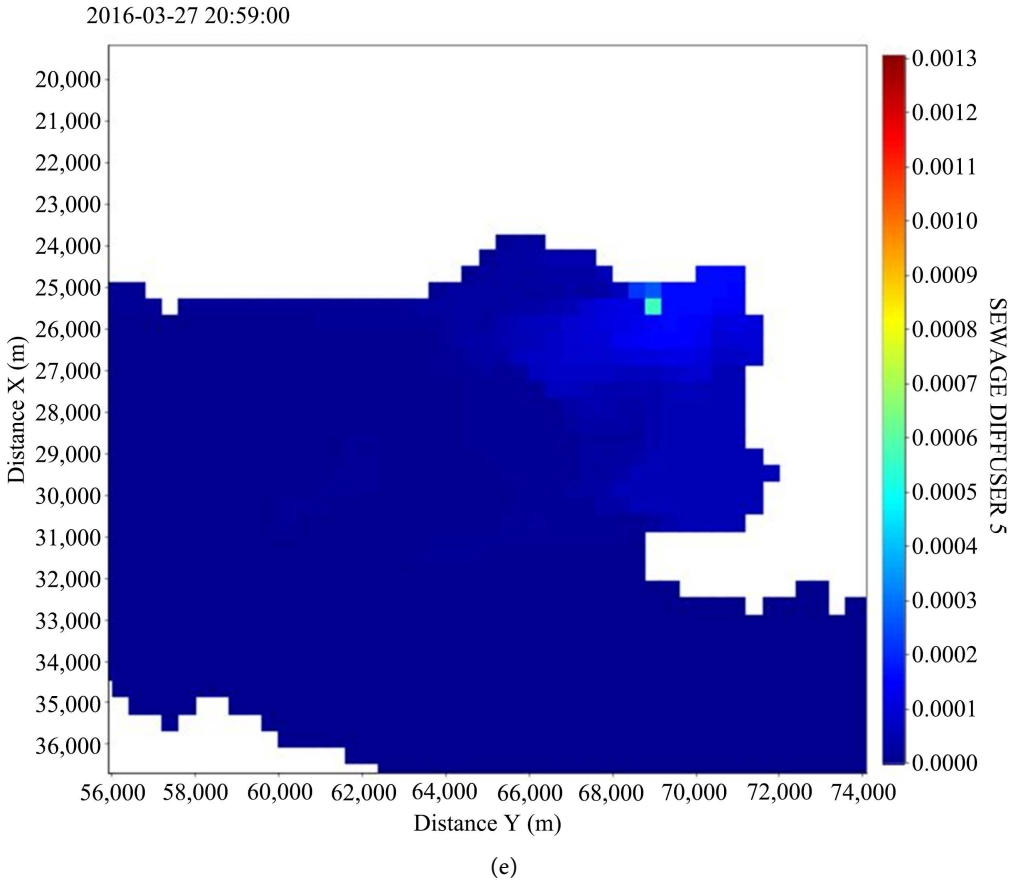

(e)

Figure 11. Color representation of the dimensionless concentration of conservative tracers from municipal wastewater disposal at various times of the simulation at the bottom, (a) TRACER 3 from DIFFUSER 1 in the KASTELA area, (b) TRACER 4 from DIFFUSER 2 in the CHALKIS area, (c) TRACER 5 from DIFFUSER 3 in the ERETRIA area, (d) TRACER 6 from DIFFUSER 4, in the AMARINTHOS area and (e) TRACER 7 from DIFFUSER 5, in the ALIVERI area.

the conservative tracers representing the liquid urban waste disposed by the diffusers at various times of the simulation on the bottom.

5. Hypothetical Climate Scenario and Results

In this paper, a hypothetical climate scenario of a future increase of the global average air temperature by 1.5˚C is considered, provided that in the next 64 years there is no reversal of the greenhouse effect, which is mainly considered responsible for this increase, and that the average air temperature continues to increase at the same rate as in previous years, as mentioned in paragraph 1. For this reason, a second simulation was performed, in which in the meteorological data that entered into the time series of air temperature values, all values was considered 1.5˚C higher than the corresponding ones of the year 2016, as illustrated in the following Figure 12. No changes were made to the values of the time series of incident solar radiation, since it was not possible to predict changes in the rate of cloud cover due to the long-term release of CO_2 and other greenhouse gases likely to affect it.

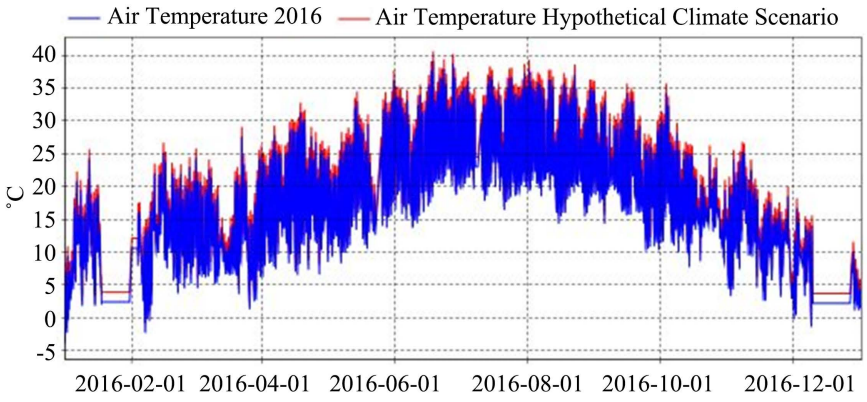

Figure 12. Comparison of air temperature per decade for the year 2016 in the study area and increased by 1.5˚C, according to the hypothetical climate scenario.

Based on the two simulations, that of the year 2016 and that of the hypothetical climate scenario, the warmest period is from 15 June to 27 August, with the warmest day being the 2nd of August, when the highest temperature of 36˚C was recorded. For this warm period, the vertical distribution of temperature and water density at three control points of coastal areas of interest (P2, P4, P5) will be examined at the hottest day of the simulations, which is the 2nd of August, in order to verify in principle, whether the future increase in average air temperature will cause a variation in the stratification of the water column at these points and, consequently, in the concentrations in the bottom layers, with regard to the conservative pollutants originating from the local urban waste water disposal systems. From the comparison of the vertical distributions of temperatures and water densities of the simulation results of the two models, on the warmest day of the simulations (2 August) for the control points P2, P4 and P5, a slightly stronger thermocline in the middle and bottom layers was found in the hypothetical climate scenario, compared to that of 2016. Specifically, a slight increase in temperature and water density of (0.5, 0.8 and 0.65)˚C in terms of temperature and (0.12, 0.22 and 0.17) Kg/m^3 in terms of water density was observed at the points (P2, P4, P5) respectively, as shown in the following **Figures 13(1a)-(1c)** and **Figures 13(2a)-(2c)**.

Density σ is related to the density ρ, through the formula:

$$\rho = 1000 + \sigma\left(\mathrm{Kg}/\mathrm{m}^3\right) \tag{1}$$

While the stratification gradient is calculated from the formula:

$$\varepsilon(z) = -(g/\rho_b)\cdot(\rho_s - \rho_b/H) \tag{2}$$

where $\varepsilon(z)$ is the stratification gradient, ρ_s is the surface density, ρ_b is the bottom density, H is the depth of water and g is the acceleration of gravity [30].

Next, they were examined comparatively for the two simulations (current and future situation): 1) The water age; 2) The dimensionless concentration of tracers representing the urban wastewater coming from the local pipelines DIFFUSER 2, DIFFUSER 4 and DIFFUSER 5; and 3) The concentrations of suspended solid

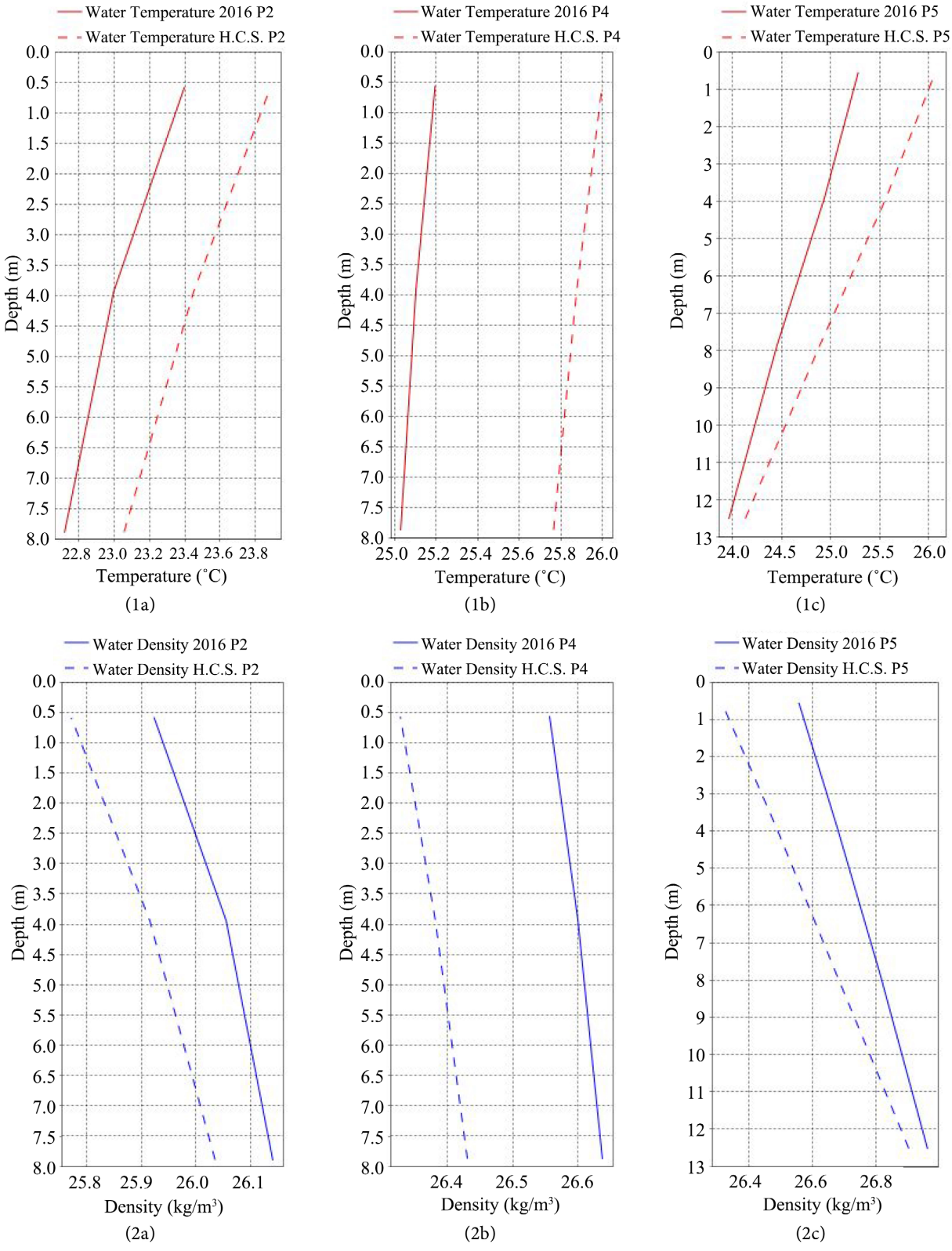

Figure 13. Comparison of the vertical distribution of 1) Temperature and 2) Water density s, as obtained from the AEM3ED software for the year 2016 and for the year of the hypothetical climate scenario (H.C.S. for short), (a) At point P2 of the CHALKIS region, (b) At point P4 of the AMARINTHOS region and (c) At point P5 of the ALIVERI region, on the hottest day of the simulations (August 2 at 11:30 a.m.).

particles contained in the disposed urban wastewater at the control points, P2 located in the CHALKIS area, P4 located in the AMARINTHOS area and P5 located in the ALIVERI area. The test was conducted for the warmest period of the simulations from 15 June to 27 August, in the bottom layers of the points, at depths of 8 m and 13 m respectively, as shown in the following Figures 14(a)-(c), Figures 15(a)-(c) and Figures 16(a)-(c).

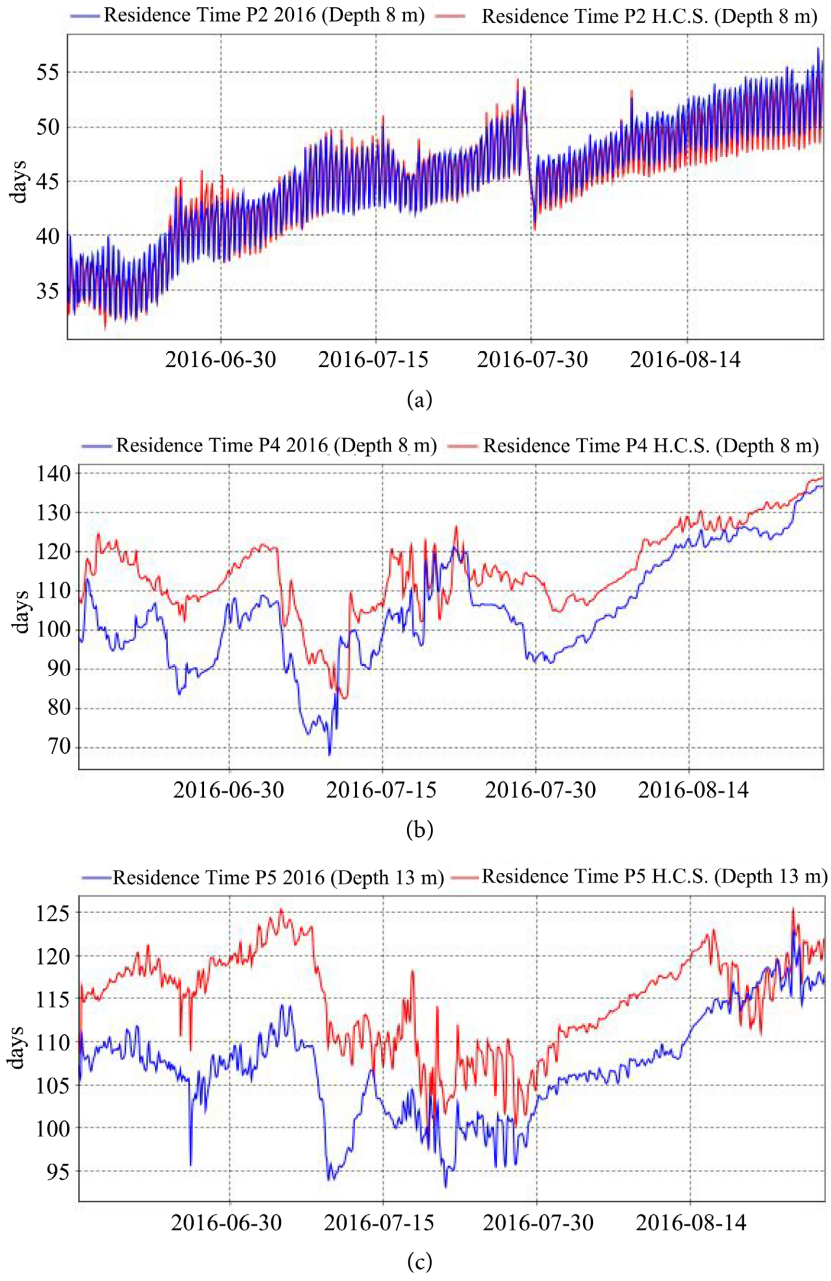

Figure 14. Comparison of the water age, during the warmest period of the simulations from 15 June to 27 August as derived from the AEM3ED software for the model of the year 2016 and for the hypothetical climate scenario (H.C.S. for short), (a) At point P2 of the CHALKIS area in the 8 m bottom layer, (b) At point P4 of the AMARINTHOS area in the 8 m bottom layer and (c) At point P5 of the ALIVERI area in the 13 m bottom layer.

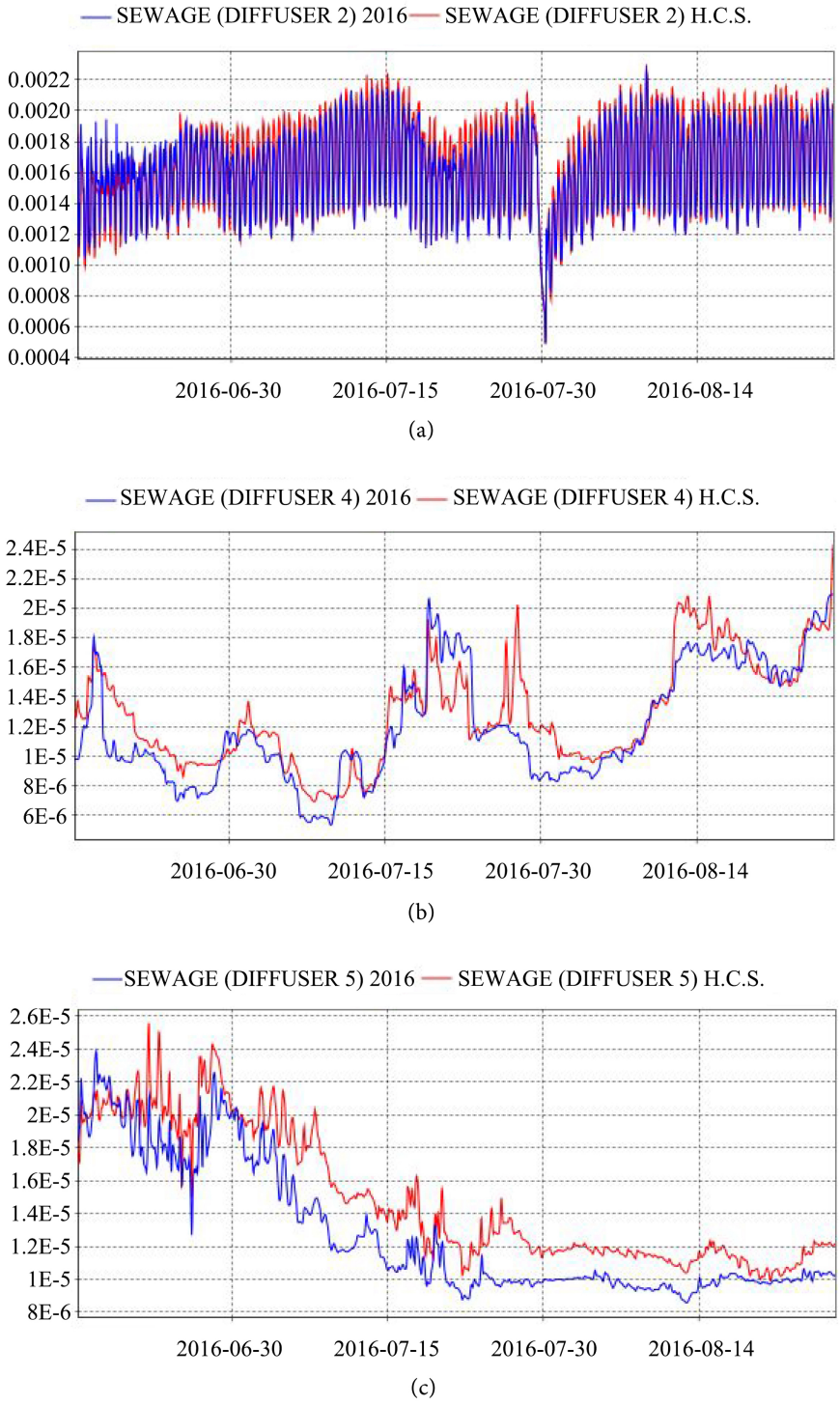

Figure 15. Comparison of the dimensionless concentration of tracers representing the wastewater coming from the local drains during the hottest period of the simulations, from 15 June to 27 August, as obtained from the simulation with the AEM3ED software for the year 2016 and for the year of the hypothetical climate scenario (H.C.S. for short), (a) TRACER 4 from DIFFUSER 2 at point P2 in the CHALKIS area at 8 m bottom layer, (b) TRACER 6 from DIFFUSER 4 at point P4 in the AMARINTHOS area at 8 m bottom layer and (c) TRACER 7 from DIFFUSER 5 at point P5 in the ALIVERI area at 13 m bottom layer.

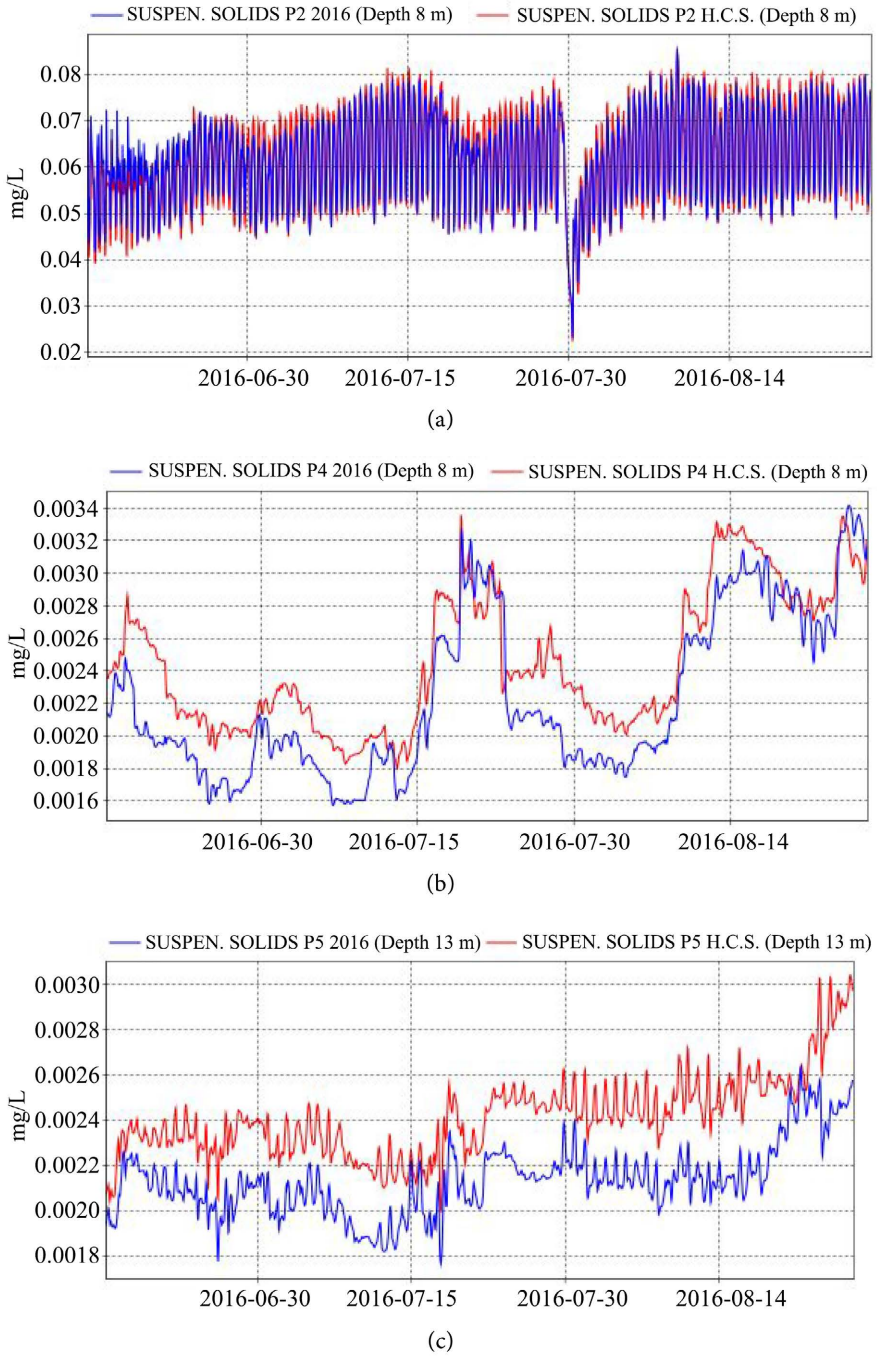

Figure 16. Comparison of suspended particulate matter concentration during the warmest period of the simulations from 15 June to 27 August, as derived with AEM3ED software for the year 2016 and for the year of the hypothetical climate scenario (H.C.S. for short), (a) At point P2 in the CHALKIS area in the 8 m bottom layer, (b) At point P4 in the AMARINTHOS area in the 8 m bottom layer and (c) At point P5 in the ALIVERI area in the 13 m bottom layer.

Figures 14-16 above show that in the 8 m and 13 m bottom layers of control points P4 and P5 respectively, between the two models, during the hottest period of the simulations, from 15 June to 27 August, where an increase in stratification

has been observed, there appear: I) An increase in the water residence time (according to Figure 14(b) and Figure 14(c)), of up to 10 days, at points P4 and P5; II) Likewise, an increase in the dimensionless concentration of tracers representing the disposed urban wastewater from the DIFFUSER 4 and DIFFUSER 5 pipelines (according to Figure 15(b) and Figure 15(c) and III) An increase in the concentration of suspended solid particles from the urban wastewater discharged (according to Figure 16(b) and Figure 16(c)) of up to 0. 003 mg/l at point P4 and 0.004 mg/l at point P5, in the model of the hypothetical climate scenario, compared to that of the year 2016. Regarding the 8 m deep bottom layer at point P2 located in the CHALKIS area, although according to Figure 13(1a) and Figure 13(2a), there is a slight increase in stratification in the model of the hypothetical climate scenario compared to the model of the year 2016, during the warmest day of the simulations (2 August), the results according to Figure 14(a), Figure 15(a) and Figure 16(a) are not similar to those of points P4 and P5. In particular, there are zero to no differences, in terms of water residence time, the dimensionless concentration of urban wastewater from the DIFFUSER 2 pipeline and the concentration of suspended solid particles, between the two models, the hypothetical and the one for the year 2016. This is apparently due to the fact that point P2, is much closer than points P4 and P5 to the Euripus Strait, which experiences strong tidal conditions with higher water velocities. This can be seen from Figure 17, which illustrates the variation in average water velocity during the warm period from 15 June to 27 August in the bottom layers of points P2, P4 and P5, at depths of 8 m, 8 m and 13 m respectively, showing a higher water velocity at point P2 than at the other two points P4 and P5. The higher velocity at point P2, leads to faster water recharge in the bottom layer and satisfactory diffusion of the wastewater from the local DIFFUSER 2.

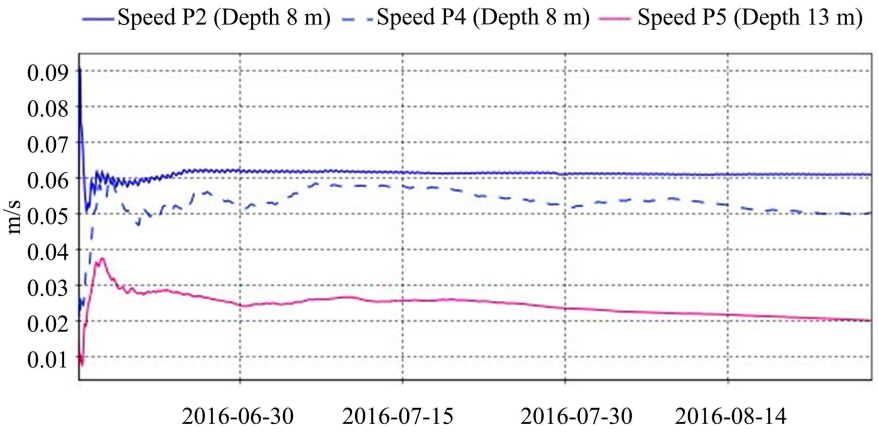

Figure 17. Comparison of the daily water speed, as derived from the AEM3ED software for the year 2016, during the warmest period of the simulation from 15 June to 27 August, between the bottom layers of the control points P2 of the CHALKIS area at a depth of 8 m, P4 of the AMARINTHOS area at a depth of 8 m and P5 of the ALIVERI area at a depth of 13 m.

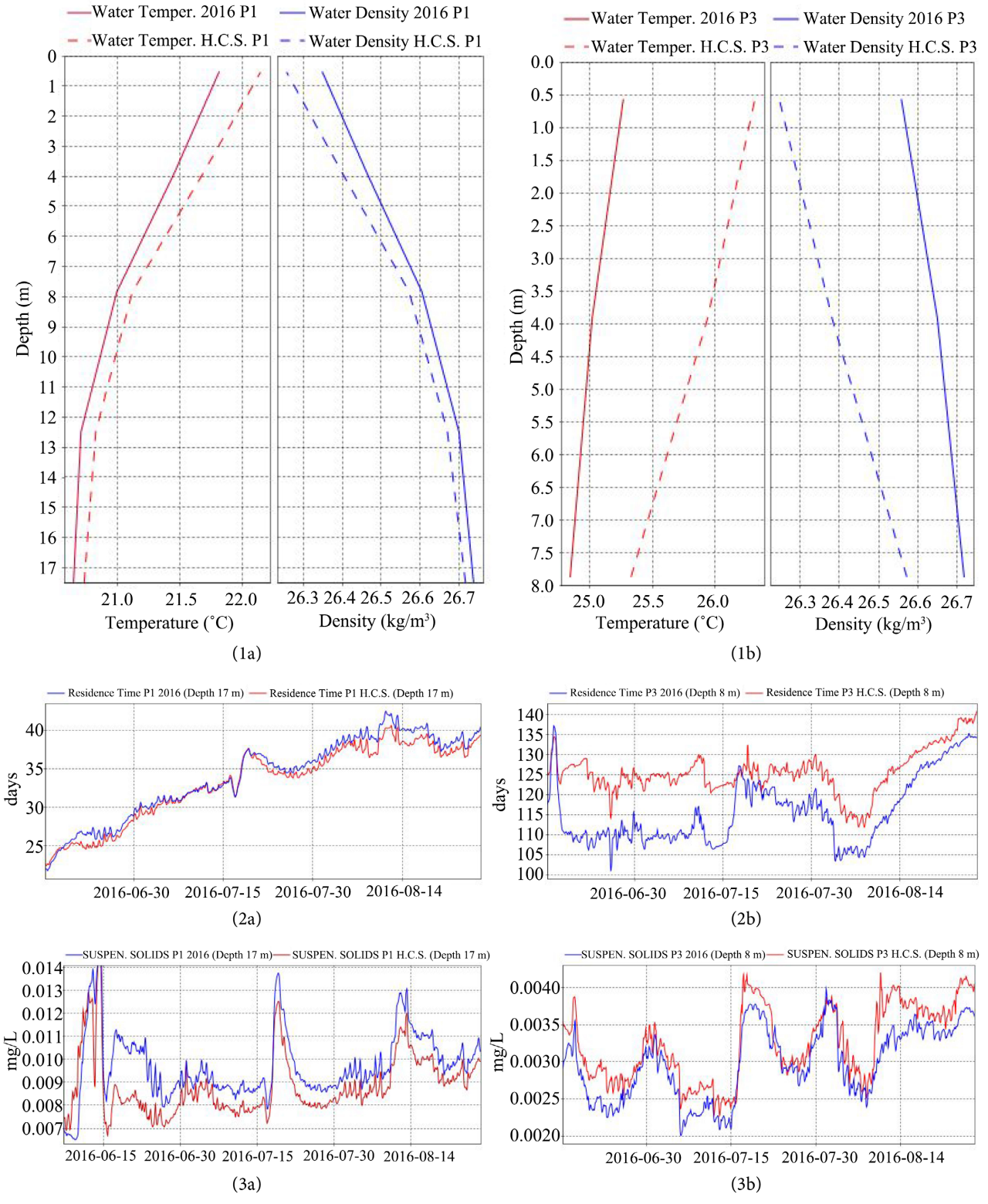

Figure 18. Comparison of 1) The vertical distributions of temperature and water density s on the hottest day of the simulations (August 2) 2) The water age during the hottest period of the simulations from June 15 to August 27 and 3) The concentration of suspended particles, similarly during the warm period of the simulations at the control points, (a) At point P1 in the POLITIKA area and (b) At point P3 in the ERETRIA area, in their bottom layers (17 m) and (8 m) respectively, between the model of the year 2016 and that of the hypothetical climate scenario (H.C.S. for short).

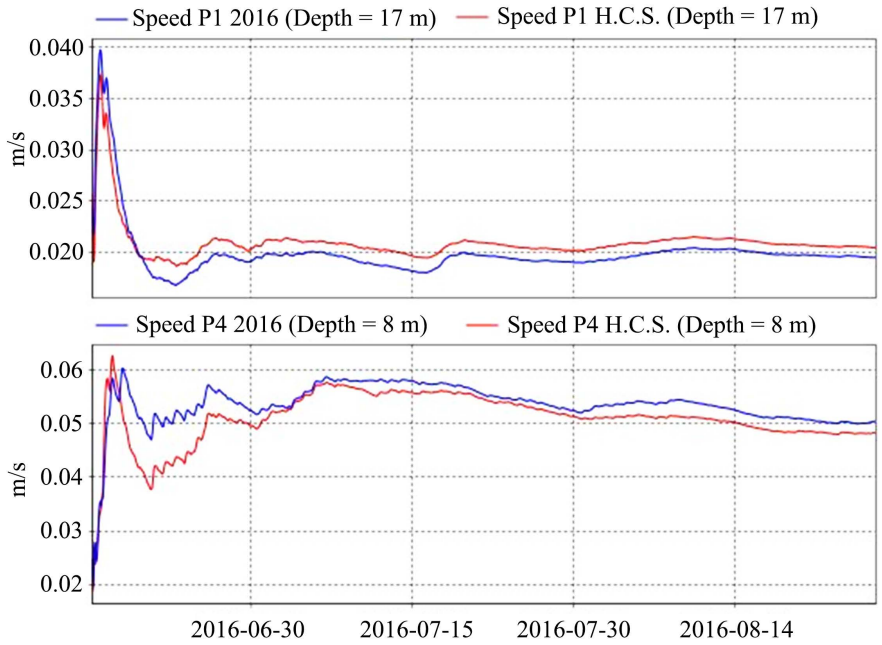

Figure 19. Comparison of the daily water speed, during the warmest period of the simulations from 15 June to 27 August as obtained from the AEM3ED software for the model of the year 2016 and for the hypothetical climate scenario (H.C.S. for short), at point P1 of the POLITIKA area in the 17 m bottom layer, and at point P4 of the AMARINTHOS area in the 8 m bottom layer.

It is also interesting to consider the comparison of the vertical distributions of temperature and water density between the 2016 model and the hypothetical climate scenario, for two other coastal areas of interest, P1 in the POLITIKA area of North Euboean Gulf and P3 in the ERETRIA area of South Euboean Gulf depicted in **Figure 10**, during the warmest day of the simulations on the 2nd of August. **Figure 18(1a)** shows for P1 that the change in the curves of the vertical distributions in temperature and water density is the same for both models. While from **Figure 18(1b)** for point P3, slightly steeper sloping distributions were obtained in the case of the hypothetical scenario compared to that of year 2016. Also as expected, the slight increase in water column temperature in the water column at point P3 leads to lower density values in the case of the hypothetical climate scenario, compared to that of the year 2016. The following is a comparison of the water residence time and the concentration of suspended solids in the bottom layers of points P1 and P3, at a depth of 17 m and 8 m respectively, between the results obtained for the hypothetical climate scenario and that of the year 2016, during the warmest period of the simulations from 15 June to 27 August, according to **Figure 18(2a)** and **Figure 18(2b)** and **Figure 18(3a)** and **Figure 18(3b)**. For point P1, a shorter water residence time is obtained in the case of the hypothetical scenario compared to that of the year 2016 (**Figure 18(2a)**), which leads to a better diffusion of the conservative pollutants to the bottom in the case of the hypothetical scenario compared to that of the year 2016, as shown in **Figure 18(3a)**. The results for point P3, as shown in **Figure**

18(2b) and Figure 18(3b) are contrary to those of point P1 and similar to those of points P4 and P5, as shown in Figure 14(b) and Figure 14(c) and Figure 16(b) and Figure 16(c). This is due to the development of higher water velocities during the warm period from 15 June to 27 August in the bottom layer of point P1 in the case of the hypothetical climate scenario compared to that of the year 2016 and lower ones during the same period in the bottom layers of the other control points (P3, P4 and P5) in the case of the hypothetical climate scenario compared to that of the year 2016, as shown representatively in Figure 19.

6. Conclusions

In this paper, the hydrodynamic circulation in the Euboean Gulf is simulated computationally with the 3-Dimensional coupled Hydrodynamic-Aquatic Ecosystem Model AEM3D, which is the evolution of the ELCOM-CAEDYM software that includes the effect of tides, the Coriolis force and climatological factors.

Two simulations were run. One used meteorological data from local measurement stations taken in the year 2016 and one of a hypothetical climate scenario, in which a time series for air temperature was used, with values higher on average by 1.5˚C, compared to those prevailing in the year 2016. A comparison of the results in terms of density in the water column at typical coastal points of interest showed an increase in stratification during the warm period of the simulations, in the hypothetical climate scenario compared to that of the year 2016. The results also showed in the bottom layers of the points of interest, longer water residence times, higher concentrations in the tracers representing urban wastewater discharged to the coastal areas from local pipelines and higher concentrations in the suspended solid particles contained in the urban wastewater, in the case of the hypothetical climate scenario, compared to that of the year 2016. Of particular interest are the coastal areas located near the Euripus Strait, where strong tides prevailing in these areas cause higher velocities and better water recharge in the bottom layers, resulting in no differentiation in the diffusion of conservative pollutants in urban wastewater between the two models, although in the hypothetical climate scenario, we have a slight increase in stratification compared to that of the year 2016. While the regions where no change in stratification is observed in future increases in global average air temperature appear to have less pollution, in the warm season, due to faster water recharge in them, due to their lower density.

The above generally indicates that the slight increase in stratification that is expected to occur in the future in the absence of greenhouse gas mitigation will further prevent the vertical mixing of the marine masses, especially in the coastal areas of the South Euboean Sea and consequently the mixing of conservative pollutants released into the coastal marine environment from anthropogenic activities. This sets the basis for further research on the application of methods to reduce stratification in areas of interest, while ensuring their water quality.

Acknowledgements

The writer is thankful to GOD almighty and highly appreciates Dr. Panagiotis Angelidis, Professor of the Department of Civil Engineering of the School of Engineering of the Democritus University of Thrace, who provides him the opportunity to conduct this Postdoctoral Research. The writer also expresses gratitude to his family for being by his side and finally thanks Dr. Ioannis Karamouzis for his spiritual support.

Conflicts of Interest

The authors declare no conflicts of interest regarding the publication of this paper.

References

[1] Pirooznia, M., Emadi, S.R. and Alamdari, M.N. (2016) The Time Series Spectral Analysis of Satellite Altimetry and Coastal Tide Gauges and Tide Modeling in the Coast of Caspian Sea. *Open Journal of Marine Science*, **6**, 258-269. https://doi.org/10.4236/ojms.2016.62021

[2] Onguene, R., *et al.* (2015) Overview of Tide Characteristics in Cameroon Coastal Areas Using Recent Observations. *Open Journal of Marine Science*, **5**, 81-98. https://doi.org/10.4236/ojms.2015.51008

[3] Manasrah, R. (2013) Tide Variation and Signals during 2000-2004 in the Northern Gulf of Aqaba, Red Sea. *Natural Science*, **5**, 1264-1271. https://doi.org/10.4236/ns.2013.512154

[4] Pous, S., Carton, X. and Lazure, P. (2012) A Process Study of the Tidal Circulation in the Persian Gulf. *Open Journal of Marine Science*, **2**, 131-140. https://doi.org/10.4236/ojms.2012.24016

[5] Vanlede, J., Coen, L. and Deschamps, M. (2014) Tidal Prediction in the Sea Scheldt (Belgium) Using a Combination of Harmonic Tidal Prediction and 1D Hydraulic Modeling. *Natural Resources*, **5**, 627-633. https://doi.org/10.4236/nr.2014.511055

[6] Jeyar, M., Chaabelasri, E.M. and Salhi, N. (2015) Computational Modeling of Tidal Effect on Wastewater Dispersion in Coastal Bays, Case of Tangier's Bay (Morocco). *Journal of Materials and Environmental Science*, **6**, 1715-1718.

[7] Vaselali, A. (2009) Modeling of Brine Waste Discharges Spreading under Tidal Currents. *Journal of Applied Sciences*, **9**, 3454-3468. https://doi.org/10.3923/jas.2009.3454.3468

[8] Abualtayef, M., Al-Najjar, H., Mogheir, Y. and Seif, A.K. (2016) Numerical Modeling of Brine Disposal from Gaza Central Seawater Desalination Plant. *Arabian Journal of Geosciences*, **9**, Article No. 572. https://doi.org/10.1007/s12517-016-2591-7

[9] Livieratos, E. (1980) The M_2 Sea-Tidal Propagation in the Evoikos Bay. *Technika Chronika*, **5**, 48-55.

[10] Eginitis, D. (1929) The Problem of the Tides of Euripus. *Astronomische Nachrichten*, **236**, 321-328. https://doi.org/10.1002/asna.19292361904

[11] Endros, A. (1915) Die Gezeiten, Seiches und Stromungen des Meeresbei Aristoteles. Sitzungsberichte der Bayerischen Akademie der Wissenschafter (Mathematical physics), Kl, 99.

[12] Sterneck, R.V. (1916) Zur Theorie der Euripus-Stromungen. Sitzungsberichte der Akademie der Wissenschafter in Wien (Abt. IIa).

[13] Defant, A. (1961) Physical Oceanography Volume II. Pergamon Press, London.

[14] Tsimplis, M.N. (1997) Tides and Sea-Level Variability at the Strait of Euripus. *Estuarine, Coastal and Shelf Science*, **44**, 91-101. https://doi.org/10.1006/ecss.1996.0128

[15] Wöppelmann, G. and Marcos, M. (2012) Coastal Sea Level Rise in Southern Europe and the Non-Climate Contribution of Vertical Land Motion. *Journal of Geophysical Research*, **117**, C01007. https://doi.org/10.1029/2011JC007469

[16] Ferrarin, C., Bellafiore, D., Sannino, G., Bajo, M. and Umgiesser, G. (2018) Tidal Dynamics in the Inter-Connected Mediterranean, Marmara, Black and Azov Seas. *Progress in Oceanography*, **161**, 102-115. https://doi.org/10.1016/j.pocean.2018.02.006

[17] Tsimplis, M.N. and Shaw, G.P. (2010) Seasonal Sea Level Extremes in the Mediterranean Sea and at the Atlantic European Coasts. *Natural Hazards and Earth System Sciences*, **10**, 1457-1475. https://doi.org/10.5194/nhess-10-1457-2010

[18] Marcos, M., Tsimplis, M.N. and Shaw, A.G.P. (2009) Sea Level Extremes in Southern Europe. *Journal of Geophysical Research: Oceans*, **114**, C01007. https://doi.org/10.1029/2008JC004912

[19] Poulos, S., Drakopoulos, P., Leontaris, S., Tsapakis, E. and Hatjiyianni, E. (2001) The Contribution of Tidal Currents in the Sedimentation of Strait of Avlida, Southern Evoikos Gulf, Greece. *Proceedings of the 9th International Congress*, Athens, 26-28 September 2001, 731-736.

[20] Kontoyiannis, H., Panagiotopoulos, M. and Soukissian, T. (2015) The Euripus Tidal Stream at Halkida/Greece: A Practical, Inexpensive Approach in Assessing the Hydrokinetic Renewable Energy from Field Measurements in a Tidal Channel. *Journal of Ocean Engineering and Marine Energy*, **1**, 325-335. https://doi.org/10.1007/s40722-015-0020-8

[21] Tsirogiannis, E., Angelidis, P. and Kotsovinos, N. (2019) Hydrodynamic Circulation under Tide Conditions at the Gulf of Evoikos, Greece. *Computational Water, Energy, and Environmental Engineering*, **8**, 57-78. https://doi.org/10.4236/cweee.2019.83004

[22] Kopasakis, K.I., Georgoulas, A.N., Angelidis, P.B. and Kotsovinos, N.E. (2012) Simulation of the Long-Term Fate of Water and Pollutants, Transported from the Dardanelles Plume into the North Aegean Sea. *Applied Ocean Research*, **37**, 145-161. https://doi.org/10.1016/j.apor.2012.04.007

[23] Kopasakis, K., Georgoulas, A., Angelidis P. and Kotsovinos, N. (2012) Numerical Modeling of the Long-Term Transport, Dispersion and Accumulation of Black Sea Pollutants into the North Aegean Coastal Waters. *Estuaries and Coasts*, **35**, 1530-1550. https://doi.org/10.1007/s12237-012-9540-9

[24] Spillman, C.M., Imberger, J., Hamilton, D.P., Hipsey, M.R. and Romero, J.R. (2007) Modelling the Effects of Po River Discharge, Internal Nutrient Cycling and Hydrodynamics on Biogeochemistry of the Northern Adriatic Sea. *Journal of Marine Systems*, **68**, 167-200. https://doi.org/10.1016/j.jmarsys.2006.11.006

[25] Alosairi, Y., Imberger, J. and Falconer, R.A. (2011) Mixing and Flushing in the Persian Gulf (Arabian Gulf). *Journal of Geophysical Research: Oceans*, **116**, C03029. https://doi.org/10.1029/2010JC006769

[26] Bird, D., Wain, D., Slavin, E., Zang, J., Luckwell, R. and Bryant, L.D. (2021) Stratification in a Reservoir Mixed by Bubble Plums under Future Climate Scenarios. *Water*, **13**, Article 2467. https://doi.org/10.3390/w13182467

[27] Kotsovinos, N. (1987) The Problem of Pollution in the Gulf of Evoikos. *Proceedings of the International Scientific Conference* "*The City of Chalkida*", Chalkida, 18 September 1987, 353-387.

[28] Skaloumpakas, K. (2011) Study of the Tidal Energy Potential at the Euripus Strait and Operating Modes through Tidal Turbine Installation. Master's Thesis, National Technical University of Athens, Athens.

[29] Tsirogiannis, E., Angelidis, P. and Kotsovinos, N. (2019) Mixing Characteristics under Tide, Meteorological and Oceanographic Conditions in the Euboean Gulf Greece. *Computational Water*, *Energy*, *and Environmental Engineering*, **8**, 99-123. https://doi.org/10.4236/cweee.2019.84007

[30] Fischer, H.B., List, E.J., Koh, R., Imberger, J. and Brooks, N.H. (1979) Mixing in Inland and Coastal Waters. Academic Press, New York.